Chinese Science Bulletin 2003 Vol. 48 No. 9 935—940

Experimental earth tidal models in considering nearly diurnal free wobble of the Earth's liquid core

SUN Heping[1], XU Jianqiao[1] & B. Ducarme[2]

1. Key Laboratory of Dynamic Geodesy, Institute of Geodesy and Geophysics, Chinese Academy of Sciences, Wuhan 430077, China;
2. Observatoire Royal de Belgique, Av. Circulaire 3, B-1180, Brussels, Belgium

Correspondence should be addressed to Sun Heping (e-mail: heping@asch.whigg.ac.cn)

Abstract **Based on the 28 series of the high precision and high minute sampling tidal gravity observations at 20 stations in Global Geodynamics Project (GGP) network, the resonant parameters of the Earth's nearly diurnal free wobble (including the eigenperiods, resonant strengths and quality factots) are precisely determined. The discrepancy of the eigenperiod between observed and theoretical values is studied, the important conclusion that the real dynamic ellipticity of the liquid core is about 5% larger than the one under the static equilibrium assumption is approved by using our gravity technique. The experimental Earth's tidal gravity models with considering the nearly diurnal free wobble of the Earth's liquid core are constructed in this study. The numerical results show that the difference among three experimental models is less than 0.1%, and the largest discrepancy compared to those widely used nowdays given by Dehant (1999) and Mathews (2001) is only about 0.4%. It can provide with the most recent real experimental tidal gravity models for the global study of the Earth's tides, geodesy and space techniques and so on.**

Keywords: Earth's nearly diurnal free wobble, global observations of superconducting gravimeters, dynamic ellipticity of liquid core, experimental earth tidal models.

DOI: 10.1360/03wd0353

The researches show that the movement instantaneous axis of the Earth's solid mantle and that of the Earth's liquid core in the space are usually not superposed due to the influence of the topography at the core-mantle boundary, this phenomenon can further induce the inverse eigenmode of the free core nutation (FCN). In the Earth's fixed coordinates, it is the nearly diurnal free wobble (NDFW)[1, 2]. Due to the existence of the FCN, the wave amplitudes of the P1, K1, ψ1 and φ1 in tidal gravity diurnal band are enhanced. In recent years, many valuable studies are developed by both home and international colleagues in theoretical modelling and practical detection in this aspect[2–4]. Based on the angular momentum equations, the eigenperiods are theoretically computed by using a numerical integration technique, the range is given as from 455.8 to 467.4 sidereal days (sd) depending on Earth's models adopted[5, 6]. However, the discrepancy of the eigenperiods between determined values in recent years based on ground based gravity and nutation observations and those in theoretical modelling is as high as 30 sd, and the differences of the FCN parameters as eigenperiods, resonant strengths and quality factots are relatively significant when using various techniques on ground at various regions. Therefore it is necessary for us to develop a deep study to the FCN phenomena by using identical technique and global distributed observations recorded with superconducting gravimeters (SG). Based on the SG data in the GGP network and collected by the International Centre of the Earth's Tides (ICET), the atmospheric perturbations are removed from observations for the first step, then the Earth tidal parameters including the amplitude factors and phase lags are determined precisely. The FCN resonance is studied and the eigenparameters are determined precisely after carrying out the oceanic loading corrections using various most recent ocean tidal models. Finally the experimental tidal gravity models with considering the resonant influence of the Earth's liquid core will be constructed for the purpose to provide the most recent reference models in the global study of the Earth's tides, geodesy, geophysics, space techniques and so on.

1 Data preparation

The cooperation observation and study of the GGP network started in 1997, the identical GWR superconducting gravimeters manufactured in USA are installed and the identical data acquisition systems are equipped for each station. The same central unit sensing and low pass filter are used before tidal gravity signals are acquired. The international standard techniques for data processing are employed[7,8]. In our researches, the 28 high precision and high sampling series of tidal gravity observations recorded with SGs at 20 stations are used for the first time. Except that station Pecny uses the spring gravimeter, all other stations use the superconducting gravimeters (SG). The double sphere SG instruments at stations Moxa, Wettzell and Sutherland are used. Table 1 shows the general information of the observational period and length at various stations. It is found from Table 1 that the total data length used in this study is about 806673.36 h (about 92.1 years). The principle consideration to include the observations recorded by a spring gravimeter at station Pecny in Czech Republic is the importance of the station location and of the data quality[9]. The careful data pre-processing is carried out, and the atmospheric pressure gravity admittances (APGA) are determined based on a regression technique between tidal gravity residuals and station pressure records. Then the gravity signals due to the change in atmospheric pressure are removed from the original tidal gravity observations using these APGA[10].

Table 1 General information: observation periods, atmospheric pressure gravity admittances and standard deviations at the GGP network

N	Station name	Observation period (y-m-d—y-m-d)	Length /d	APGA[a] /m • s^{-2} • hPa^{-1}	SD[b] /m • s^{-2}
1	Bandung/Indonisia	1997-12-19—1999-12-31	419.458	$(-3.52388\pm 0.24265)\times10^{-9}$	7.450×10^{-9}
2	Brussels/Belgium	1982-04-21—2000-08-21	6660.500	$(-3.46703\pm 0.00487)\times10^{-9}$	1.743×10^{-9}
3	Boulder/USA	1998-01-10—2001-05-31	1225.500	$(-3.56787\pm 0.01739)\times10^{-9}$	2.469×10^{-9}
4	Brasimone/Italy	1992-08-01—2000-02-01	1427.500	$(-3.01877\pm 0.03039)\times10^{-9}$	2.954×10^{-9}
5	Cantley/Canada	1989-11-07—1999-09-30	2386.583	$(-3.29287\pm 0.00579)\times10^{-9}$	1.443×10^{-9}
6	Canberra/ Australia	1997-07-01—1999-12–31	890.083	$(-3.39208\pm 0.01031)\times10^{-9}$	0.776×10^{-9}
7	Esashi/Japan	1997-07-01—1999-12-31	875.125	$(-3.54941\pm 0.01087)\times10^{-9}$	1.286×10^{-9}
8	Kyoto/Japan	1997-07-01—1999-12-31	686.208	$(-3.18324\pm 0.03823)\times10^{-9}$	3.323×10^{-9}
9	Matsushiro/Japan	1997-05-01—1999-12-31	880.542	$(-4.64847\pm 0.00847)\times10^{-9}$	0.954×10^{-9}
10	Membach/Belgium	1995-08-04—2000-05-31	1727.958	$(-3.28637\pm 0.00591)\times10^{-9}$	1.007×10^{-9}
11	Metsahovi/Finland	1994-08-11—2000-06-30	1614.292	$(-3.65359\pm 0.00698)\times10^{-9}$	1.299×10^{-9}
12	Moxa/Germany/lo[c]	2000-01-01—2001-08-31	579.167	$(-3.30067\pm 0.00645)\times10^{-9}$	0.536×10^{-9}
13	Moxa/ Germany /up[d]	2000-01-01—2001-08-31	580.500	$(-3.34005\pm 0.00767)\times10^{-9}$	0.638×10^{-9}
14	Moxa/ Germany /all[e]	2000-01-01—2001-08-31	1159.667	$(-3.32027\pm 0.00502)\times10^{-9}$	0.590×10^{-9}
15	Pecny/ Czech Republic	1997-10-31—1999-01-03	412.167	$(-4.89444\pm 0.01312)\times10^{-9}$	0.887×10^{-9}
16	Potsdam/Germany	1992-06-30—1998-10-08	2250.083	$(-3.31310\pm 0.00420)\times10^{-9}$	0.855×10^{-9}
17	Strasbourg/France/od[f]	1987-07-11—1996-06-25	3272.042	$(-3.12839\pm 0.00991)\times10^{-9}$	2.265×10^{-9}
18	Strasbourg/France/nw[g]	1997-03-01—1999-07-31	816.708	$(-3.39355\pm 0.00740)\times10^{-9}$	0.797×10^{-9}
19	Sutherland/ South African /lo	2000-03-27—2001-08-01	492.375	$(-2.86645\pm 0.01679)\times10^{-9}$	0.656×10^{-9}
20	Sutherland/ South African /up	2000-09-30—2001-08-01	305.208	$(-2.71681\pm 0.02272)\times10^{-9}$	0.678×10^{-9}
21	Sutherland/ South African /all	2000-03-27—2001-08-01	797.583	$(-2.81170\pm 0.01360)\times10^{-9}$	0.671×10^{-9}
22	Syowa/ South Pole	1997-07-01—1998-12-31	548.333	$(-4.11511\pm 0.00934)\times10^{-9}$	1.103×10^{-9}
23	Vienna/ Austria	1997-07-01—1999-06-30	729.333	$(3.46701\pm 0.00710)\times10^{-9}$	0.662×10^{-9}
24	Wettzell/Germany/od	1996-07-28—1998-09-23	726.042	$(-3.37353\pm 0.03087)\times10^{-9}$	2.639×10^{-9}
25	Wettzell/ Germany /lo	1998-11-04—2001-08-31	290.750	$(-3.43418\pm 0.00997)\times10^{-9}$	0.544×10^{-9}
26	Wettzell/ Germany /up	1998-11-04—2001-08-31	290.792	$(-3.24539\pm 0.01346)\times10^{-9}$	0.734×10^{-9}
27	Wettzell/ Germany /all	1998-11-04—2001-08-31	581.500	$(-3.33987\pm 0.00865)\times10^{-9}$	0.667×10^{-9}
28	Wuhan/China	1997-12-20—2000-08-31	985.333	$(-3.23704\pm 0.01066)\times10^{-9}$	0.750×10^{-9}

a) APGA denotes the atmospheric pressure gravity admittances; b) SD is standard deviations; c) lo represents the observations with lower sphere ; d) up those recorded with upper sphere ; e) all are the observations after averaging process recorded with both upper and lower sphers; f) od is the old observation series; g) nw is the new observation series at the same station.

In order to provide conveniently the necessary evaluation and comparison to the observation quality at various stations, the standard deviations (SD) of the tidal gravity parameters obtained from the data analysis are also listed in Table 1. It shows that the lower the standard deviations are, the lower the station background noise and the higher the observation quality will be.

During the data processing, the observation residuals are obtained by subtracting synthetic modelling signals from the tidal gravity records, the perturbation components in residual series as peaks, impulses, earthquakes, steps and so on are eliminated using PC visual plate provided by Tsoft[11]. The short term interruptions due to the electricity supply and instrumental broken are filled using tidal gravity synthetic modelling signals at the same station. The tidal gravity observations after perturbation corrections are obtained based on the remove-restore technique, the hourly data are then obtained after the filtering process[10, 12]. As the selected data length for all stations is longer than one year, it is possible to separate accurately 13 wave components in diurnal band including some small waves as ψ_1 and φ_1 with which the resonance signal of the Earth's liquid core is included.

The influence of the oceanic tides is one of the most important perturbations in tidal gravity observations. The

research shows that the effect of the ocean tides on gravity field can be separately into three parts, i.e. the direct attraction due to the change of the ocean tidal mass, the deformation influence of the elastic Earth under the action of the mass loads and the additional contribution induced by the mass redistribution in the interior of the Earth due to the Earth's deformation[13]. The global ocean models used for loading correction in this study include the Schwiderski's one, and those developed from the Topex/Poseidon altimeters and those result from finite element modelling, such as the CSR3.0 (Eanes), FES95.2 (Grenoble), TPXO2 (Egbert), CSR4.0 and ORI96 (Matsumoto) models[1)] and regional tidal models in China[14]. Based on the model Earth Green's functions and Agnew's loading computation technique[13,15], the influences of the ocean tides on gravity field for 8 main waves (Q1, O1, P1, K1, N2, M2, S2 and K2) are calculated. The loading vectors for other 9 additional small components as σ1, ρ1, NO1, π1, ψ1, φ1, θ1, J1 and OO1 in diurnal wave band are interpolated using an interpolation technique[16]. The core resonance phenomena on oceanic tides are taken into account during the interpolation process[6]. The efficiency of the loading correction for both principal and small tidal components are confirmed by Ducarme et al.[9] and Sun et al.[14].

2 Calculation techniques

The research shows that the complex amplitude factor with frequency σ in diurnal wave band can be theoretically computed using the formula given as[1, 2]

$$\delta_{th}(\sigma) = \delta_0 + \frac{\bar{A}}{\sigma - \bar{\sigma}_{\mathrm{FCN}}}, \tag{1}$$

with

$$\begin{aligned} \delta_0 &= 1 + h_0 - \frac{3}{2}k_0, \\ \bar{A} &= -(A/A_m)\left(h_1 - \frac{3}{2}k_1\right)(\alpha - q_0 h^c/2)\Omega, \end{aligned} \tag{2}$$

where δ_0 is the amplitude factor combined from the classical Love numbers h_0 and k_0, it is not influenced by the FCN resonance, h_1 and k_1 are the internal pressure Love numbers, h^c is the secular Love number, A and A_m are the equatorial inertia moments of the entire Earth and solid mantle, α is the dynamic ellipticity of the Earth, q_0 ratio of the centrifugal force to gravity on the equator and Ω is the sidereal frequency of the Earth's rotation. $\bar{A}$ is the complex resonance strength related to the Earth's geometric shape and the fluid properties of the Earth's mantle and $\bar{\sigma}_{\mathrm{FCN}}$ is the complex eigenfrequency, they are given as

$$\bar{A} = A_r + iA_i, \quad \bar{\sigma}_{\mathrm{FCN}} = \sigma_r + i\sigma_i, \tag{3}$$

then the FCN eigenperiod is given $T_{\mathrm{FCN}} = \Omega/(\sigma_r + \Omega)$ and the quality factor $Q = \sigma_r/(2\sigma_i)$.

Considering the high observation precision of the O1 wave and it is little influenced by the resonance (at the level of 10^{-4}) since its frequency is far away from the one of the FCN, it can be referred to as a reference. In order to reduce the influence of the systematic errors in observations and local environmental disturbances around station on the fitting parameters, the tidal signal of the O1 wave is removed from both sides of eq. (1) according to the given theoretical tidal amplitude factors, then the model used to calculate FCN fitting parameters can be obtained as

$$\delta(\sigma, j) - \delta(O_1, j) = \frac{A_r + iA_i}{\sigma - (\sigma_r + i\sigma_i)} - \frac{A_r + iA_i}{\sigma(O_1) - (\sigma_r + i\sigma_i)}, \tag{4}$$

where j stands for the station series number. To solve the above equation group, the real and imaginary parts of the complex resonant strength and complex eigenfrequency are obtained, the eigenperiod and quality factors can then be further calculated.

3 Numerical results and discussions

In order to consider the local ocean characteristics and other influences at various regions, the average process is carried out to the loading effect obtained when using 6 different global oceanic tidal models. The loading corrections to the observation results for the several waves in diurnal band (as O1, P1, K1, ψ1 and φ1) are carried out. In order to determine precisely the effect of the FCN resonance, all the 28 series observations at 20 GGP stations are stacked. The T_{FCN} numerical results are obtained in considering three cases as follows: (1) T_{FCN} is given as 429.9 sd with error range (427.2, 432.7 sd) when staking all tidal gravity observations with rejecting those recorded at stations Bandung and Kyoto since their high noise level; (2) T_{FCN} is given as 429.1 sd with error range (428.0, 430.3) when staking all tidal gravity observations (average ones after the process are adopted for the double spheres SGs, and two series as new and old ones at stations Strasbourg and Wettzell are used) with rejecting some special bad waves as K1 (Syowa), O1 (Syowa, Wettzell), P1 (Syowa), ψ1 (Bandung, Brasimone, Kyoto, Matsushir, Pecny, Sutherland), φ1 (Brasimone, Boulder, Kyoto) due to their significant noise; and (3) 429.7 sd with error range (426.8, 432.6) when taking the same procedure as (2) with considering the improvement of the signal to noise ratio by normalizing the standard deviations of the waves using the theoretical amplitudes of the corresponding waves.

1) IERS Standards, IERS technical note, Observatory of Paris, 1992(13): 1—20.

Table 2 Comparison of the tidal gravity models in the diurnal wave band

Wave argument		Frequency/(°) • h^{-1}	Name	DDW1[a)]	DDW2[b)]	MATH[c)]	SXD1[d)]	SXD2[e)]	SXD3[f)]
1-4 0 3 0 0	115.855	12.30991148	308	1.15254	1.15400		1.15473	1.15474	1.15474
1-4 2 1 0 0	117.655	12.38276513	SGQ1	1.15256	1.15402	1.15403	1.15473	1.15473	1.15473
1-3 0 1 0 0	125.655	12.84964437	no name	1.15269	1.15415		1.15468	1.15468	1.15468
1-3 0 2-1 0	125.745	12.85207978	2Q1x	1.15269	1.15415		1.15468	1.15468	1.15468
1-3 0 2 0 0	125.755	12.85428619	2Q1	1.15269	1.15415	1.15409	1.15468	1.15468	1.15468
1-3 2 0-1 0	127.545	12.92493343	SG1x	1.15271	1.15417		1.15467	1.15467	1.15467
1-3 2 0 0 0	127.555	12.92713984	SIG1	1.15271	1.15417	1.15410	1.15467	1.15467	1.15467
1-2 0 0-1 0	135.545	13.39181267	no name	1.15279	1.15425		1.15459	1.15459	1.15459
1-2 0 0 0 0	135.555	13.39401908	no name	1.15279	1.15425		1.15458	1.15459	1.15459
1-2 0 1-1 0	135.645	13.39645449	Q1x	1.15279	1.15425	1.15410	1.15458	1.15459	1.15459
1-2 0 1 0 0	135.655	13.39866089	Q1	1.15280	1.15425	1.15410	1.15458	1.15459	1.15459
1-2 2-1 0 0	137.455	13.47151455	RHO1	1.15280	1.15426	1.15410	1.15457	1.15457	1.15457
1-1 0 0-1 0	145.545	13.94082919	O1x	1.15279	1.15424	1.15401	1.15440	1.15440	1.15440
1-1 0 0 0 0	145.555	13.94303560	O1	1.15279	1.15424	1.15401	1.15440	1.15440	1.15440
1-1 0 1 0 0	135.655	13.94767741	no name	1.15279	1.15424		1.15440	1.15440	1.15440
1-1 0 2 0 0	145.755	13.95231923	2NO1	1.15279	1.15424		1.15440	1.15440	1.15440
1-1 2 0 0 0	147.555	14.02517288	TAU1	1.15278	1.15422	1.15397	1.15436	1.15436	1.15436
1 0-2 1 0 0	153.655	14.41455665	NTAU	1.15252	1.15396	1.15366	1.15400	1.15399	1.15399
1 0 0-1-1 0	155.445	14.48520390	LK1x	1.15242	1.15386		1.15388	1.15387	1.15387
1 0 0-1 0 0	155.455	14.48741031	LK1	1.15242	1.15385	1.15354	1.15388	1.15387	1.15387
1 0 0 0-1 0	155.545	14.48984571	no name	1.15242	1.15385		1.15387	1.15386	1.15386
1 0 0 0 0 0	155.555	14.49205212	no name	1.15241	1.15385		1.15387	1.15386	1.15386
1 0 0 0 1 0	155.565	14.49425853	no name	1.15241	1.15384		1.15386	1.15386	1.15386
1 0 0 1 0 0	155.655	14.49669393	NO1	1.15240	1.15384	1.15351	1.15386	1.15385	1.15385
1 0 0 1 1 0	155.665	14.49890034	NO1x	1.15240	1.15383	1.15351	1.15386	1.15385	1.15385
1 0 2-1 0 0	157.455	14.56954759	CHI1	1.15226	1.15369	1.15336	1.15370	1.15369	1.15369
1 1-3 0 0 1	162.556	14.91786468	PI1	1.14933	1.15072	1.15043	1.15091	1.15087	1.15087
1 1-2 0-1 0	163.545	14.95672495	P1x	1.14788	1.14927	1.14903	1.14959	1.14953	1.14953
1 1-2 0 0 0	163.555	14.95893136	P1	1.14777	1.14916	1.14892	1.14949	1.14943	1.14942
1 1-1 0 0 1	164.556	15.00000196	S1	1.14446	1.14589	1.14578	1.14654	1.14643	1.14643
1 1 0-1 0 0	165.455	15.03642683	no name	1.13543	1.13728		1.13879	1.13860	1.13858
1 1 0 0-1 0	165.545	15.03886223	K1x-	1.13416	1.13610	1.13610	1.13773	1.13753	1.13751
1 1 0 0 0 0	165.555	15.04106864	K1	1.13284	1.13489	1.13494	1.13664	1.13643	1.13641
1 1 0 0 1 0	165.565	15.04327505	K1x+	1.13133	1.13352	1.13361	1.13541	1.13518	1.13516
1 1 1 0 0-1	166.554	15.08213532	PSI1	1.23736	1.26978	1.26548	1.25993	1.26302	1.26217
1 1 2 0 0 0	167.555	15.12320592	PHI1	1.16776	1.17029	1.16932	1.16856	1.16878	1.16876
1 2-2 1 0 0	173.655	15.51258969	TET1	1.15551	1.15703	1.15641	1.15643	1.15646	1.15646
1 2 0-1 0 0	175.455	15.58544335	J1	1.15531	1.15682	1.15619	1.15622	1.15625	1.15625
1 2 0-1 1 0	175.465	15.58764975	J1x	1.15530	1.15682	1.15618	1.15622	1.15624	1.15624
1 2 0 0 0 0	175.555	15.59008516	no name	1.15530	1.15681		1.15621	1.15624	1.15624
1 2 0 0 1 0	175.565	15.59229157	no name	1.15529	1.15681		1.15621	1.15623	1.15623
1 3-2 0 0 0	183.555	16.05696440	SO1	1.15482	1.15631	1.15559	1.15562	1.15564	1.15564
1 3 0-2 0 0	185.355	16.12981805	2J1	1.15479	1.15628		1.15557	1.15559	1.15559
1 3 0-1 0 0	185.455	16.13445987	no name	1.15479	1.15628		1.15557	1.15559	1.15559
1 3 0 0 0 0	185.555	16.13910168	OO1	1.15479	1.15628	1.15555	1.15557	1.15559	1.15559
1 3 0 0 1 0	185.565	16.14130809	OO1x	1.15479	1.15628	1.15555	1.15557	1.15558	1.15558
1 4 0-1 0 0	195.455	16.68347639	NU1	1.15474	1.15623	1.15538	1.15536	1.15538	1.15538
1 4 0-1 1 0	195.465	16.68568279	NU1x	1.15474	1.15623		1.15536	1.15538	1.15538

a) DDW1: Theoretical Earth tidal models in hydrostatic hypotheses (Dehant et al., 1999)[17]; b) DDW2: theoretical Earth tidal models in non-hydrostatic hypotheses (Dehant et al., 1999)[17]; c) MATH: theoretical Earth tidal models including VLBI observations (Mathews, 2001)[6]; d) SXD1: experimental Earth tidal models given by Sun-Xu-Ducarme in this paper; e) SXD2: experimental Earth tidal models given by Sun-Xu-Ducarme in this paper; f) SXD3: experimental Earth tidal models given by Sun-Xu-Ducarme in this paper.

The above numerical results show that the resonant eigenperiods T_{FCN} of the Earth's liquid core determined when using global SG observations in our study are very close to the one (429.5 sd) given in theoretical computation by Dehant[17] and the one (430.04 sd) obtained when using VLBI observations with considering the electromagnetic coupling force at the core-mantle boundary by Mathews[16], the largest discrepancy is only 0.4%. However it is found that there exists a discrepancy when comparing our results with those obtained in early ground based tidal gravity observations[1–4]. Furthermore, it should be pointed out that the discrepancy is as large as 30 sd when comparing all ground based experimental results with those given by theoretical computations by Wahr and Sasao[5], therefore it is necessary for us to search deeply the reasons for such a discrepancy.

As a matter of fact, the early study shows that the FCN resonant parameters depend mainly upon the Earth's structural, the physical and mechanical properties. Based on an Earth model with an elastic solid mantle, a fluid outer core and an elastic solid inner core, the analytical expression of the FCN eigenfrequency σ_{FCN} ($\sigma_{\mathrm{FCN}}=1/T_{\mathrm{FCN}}$) can be given approximately as

$$\sigma_{\mathrm{FCN}} = -\left[1+\frac{A-A_I}{A_m}(e_f-\beta)\right]\Omega, \qquad (5)$$

where e_f is the dynamic ellipticity of the Earth's liquid core (at the order of 10^{-3}), β is a small parameter describing the elastic deformation of the mantle (at the order of 6.27×10^{-4}), A, A_I and A_m are the equatorial inertia moments of the whole Earth, mantle and solid inner core. Among them A_I is only at the level 10^{-4} of the A. The earlier theoretical studies indicate that in assumption of the hydrostatic equilibrium, only a few days discrepancy on the T_{FCN} for various Earth models is found. The present discrepancies between the observed tidal gravity amplitude factors and those given in theoretical tidal modelling are less than 0.4% which implies that the real Earth's deformation can be well approximated by the recent Earth's deformation theory. From formula (5), the dynamic ellipticity of the Earth's fluid core e_f can then be calculated when having high precision FCN eigenfrequency. Based on our numerical results, the reasonable explanation to the 30 sd less of the observed eigenperiod than the one in theoretical computation is that the real dynamic ellipticity of the Earth's liquid core is about 5% larger than the one given under the hydrostatic equilibrium assumption.

Based on the T_{FCN} numerical results in the above cases and formula (1), three experimental Earth tidal models as SXD1, SXD2 and SXD3 including the influence of the FCN resonance are constructed (Table 2). The numerical results show that the discrepancy among amplitude factors in three experimental models is less than 0.1% (Table 2 and Fig. 1). Fig. 2 shows the intercomparison among three experimental models with the theoretical one given by Mathews in which the VLBI observations is considered. It shows that the largest discrepancy is located near the FCN resonant frequency and they are 0.56% (SXD1), 0.25% (SXD2) and 0.33% (SXD3). The widely used DDW standard theoretical tidal models given by Dehant are also listed in Table 2 for the easy comparison. The numerical results demonstrate that three experimental models given in this report are very close to the theoretical ones given in DDW and Mathews. Considering that the discrepancy for SXD2 model when compared to the one in Mathews is lowest, it proves that this model is a little bit better than others, it also shows the effectiveness of rejecting some bad waves.

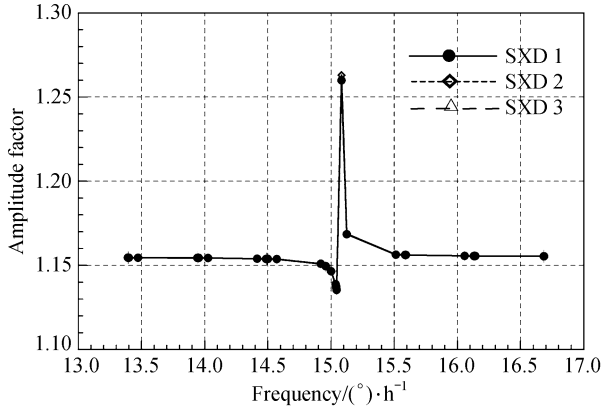

Fig. 1. Comparison of the amplitude factors among three SXD models.

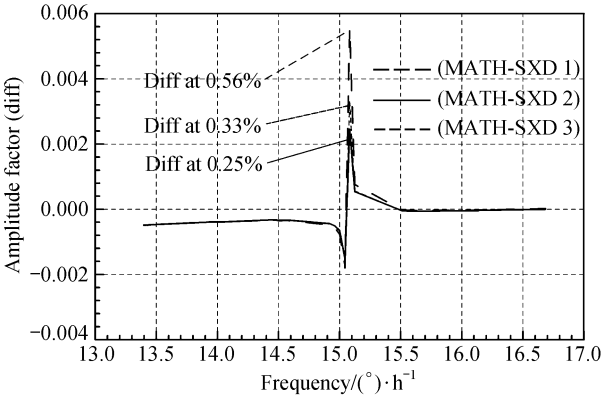

Fig. 2. Comparison between the experimental tidal gravity models and those given by Mathews.

4 Conclusions

Based on the numerical results and discussions mentioned above, the global distributed high precision tidal gravity observations are the important assurance in determining the FCN resonant parameters. The reasonable explanations for about 30 sd less of the determined FCN

eigenperiod in this report than the one in theoretical value are discussed. The important conclusion in which the real dynamic ellipticity of the Earth's fluid core is about 5% larger than the one given under the assumption of the hydrostatic equilibrium is approved by using the gravity technique. The experimental Earth tidal models constructed when including the resonance influence of Earth's liquid core, are in good agreement with those in theoretical computations, they can be provided as the newest tidal gravity experimental models in the global study of the Earth tides, geodesy, geophysics, space techniques and so on.

Acknowledgements We are grateful to the GGP Chairman, Crossley and observation staff members at all stations in GGP network for their effort to acquire high precision data. The authors wish to express their thanks to J. C. Zhou from Institute of Geodesy and Geophysics participated in the ocean loading computation, M. Hendrickx and L. Vandercoilden from Royal Observatory of Belgium participated in the SG data analysis. This work was supported jointly by the National Outstanding Youth Science Foundation of China (Grant No. 49925411), the Knowledge Innovation Project of the Chinese Academy of Sciences (Grant No. KZCX3-CW-131) and the National Natural Science Foundation of China (Grant No. 40174022).

References

1. Herring, T. A., Gwinn, C. R., Shapiro, I. I., Geodesy by radio interferometry: studies of the forced nutations of the Earth 1. data analysis, Journal of Geophysical Research, 1986, 91(B5): 4745—4754.
2. Defraigne, P., Dehant, V., Hinderer, J., Staking gravity tide measurements and nutation observations in order to determine the complex eigenfrequency of nearly diurnal free wobble, Journal of Geophysical Research, 1994, 99(B5): 9203—9213.
3. Sato, T., Fluid core resonance measured by quartz tube extensometers at Esashi Earth tide station (ed. Kakkuri, J.), Proc. of 11th Int. Sympos. Earth Tides, Stuttgart: E. Schweizerbart'sche, 1991, 573—582.
4. Xu, J. Q., Sun, H. P., Luo, S. C., Study of the Earth's free core nutation by tidal gravity data recorded with international superconducting gravimeters, Science in China, Series D, 2002, 45(4): 337—347.
5. Wahr, J. M., Sasao, T., A diurnal resonance in the ocean tide and in the Earth's load response duo to the resonant free core nutation, Geophys. J. R. astr. Soc. 1981, 64: 747—765.
6. Mathews, P. M., Love numbers and gravimetric factor for diurnal tides, Journal of the Geodetic Society of Japan, 2001, 47(1): 231—236.
7. Crossley, D. J., Hinderer, J., Global geodynamics project-GGP: status report 1994, Proc. of workshop on non-tidal gravity changes, Luxembourg: Conseil de L'Europe Cahiers du Centre Européen de Géodynamique et de Séismologie (ed. Poitevin, C.), 1995, 11: 244—269.
8. Wenzel, H. G., The nanogal software: data processing package Eterna 3.3, Bulletin D'informations de Marées Terrestres, 1996, 124: 9425—9439.
9. Ducarme, B., Sun, H. P., Xu, J. Q., New investigation of tidal gravity results from the GGP Network, Bulletin D'informations de Marées Terrestres, 2002, 136: 10761—10775.
10. Sun, H. P., Takemoto, S., Hsu, H. T. et al., Precise tidal gravity recorded with superconducting gravimeters at stations Wuhan/China and Kyoto/Japan, Journal of Geodesy, 2001, 74: 720—729.
11. Vauterin, P., Tsoft: graphical and interactive software for the analysis of earth tide data, Proc. of 13th Int. Sympos. Earth Tides (eds. Paquet, P., Ducarme, B.), Brussels: Observatoire Royal de Belgique, Série Géophysique, 1998, 481—486.
12. Chen, X. D., Sun, H. P., New method for pre-processing and analyzing tidal gravity observations, Journal of Geodesy and Geodynamics (in Chinese), 2002, 22(3): 83—87.
13. Sun, H. P., Comprehensive researches for the effect of the ocean loading on gravity observations in the western Pacific area, Bulletin D'informations de Marées Terrestres, 1992, 113: 8271—8292.
14. Sun, H. P., Xu, H. T., Jentzsch, G. et al., Tidal gravity observations obtained with a superconducting gravimeter at Wuhan/China and its application to geodynamics, Journal of Geodynamics, 2002, 33(1–2): 187—198.
15. Agnew, D. C., A program for computing ocean-tide loading, Journal of Geophysical Research, 1997, 102(B3): 5109—5110.
16. Sun, H. P., Xu, J. Q., Ducarme, B., Experimental Earth tidal models of the core resonance obtained by stacking tidal gravity observations from GGP Stations, Bulletin D'informations de Marées Terrestres, 2002, 136: 10729—10733.
17. Dehant, V., Defraigne, P., Wahr, J., Tides for a convective Earth, Journal of Geophysical Research, 1999, 104(B1): 1035—1058.

(Received January 22, 2003; accepted March 17, 2003)